Dispersion and attenuation due to scattering from heterogeneities of the frame bulk modulus of a poroelastic medium

Brian T. Hefner and Darrell R. Jackson

Applied Physics Laboratory,

University of Washington,

1013 NE 40th St,

Seattle,

WA 98105

(Dated: February 19, 2010)

ONR Award # N00014-05-1-0025

REPORT DOCUMENTATION PAGE

Form Approved
OMB No. 0704-0188

PLEASE DO NOT RETURN YOUR FORM TO THE ABOVE ADDRESS.

1. REPORT DATE *(DD-MM-YYYY)*	2. REPORT TYPE	3. DATES COVERED *(From - To)*
02-19-2010	Final Report	15 January 2005 - 31 December 2009

4. TITLE AND SUBTITLE

Dispersion and attenuation due to scattering from heterogeneities of the frame bulk modulus of a poroelastic medium

5a. CONTRACT NUMBER

5b. GRANT NUMBER

N00014-05-10025

5c. PROGRAM ELEMENT NUMBER

6. AUTHOR(S)

Brian T. Hefner, University of Washington
Darrell R. Jackson, University of Washington

5d. PROJECT NUMBER

5e. TASK NUMBER

5f. WORK UNIT NUMBER

7. PERFORMING ORGANIZATION NAME(S) AND ADDRESS(ES)

Applied Physics Laboratory
University of Washington
1014 NE 40th St.
Seattle, WA 98105

8. PERFORMING ORGANIZATION REPORT NUMBER

9. SPONSORING/MONITORING AGENCY NAME(S) AND ADDRESS(ES)

Dr. Robert Headrick, Code 321OA
Office of Naval Research
1107 NE 45th St.
Suite 350
Seattle, WA 98105-4631

10. SPONSOR/MONITOR'S ACRONYM(S)

ONR

11. SPONSOR/MONITOR'S REPORT NUMBER(S)

12. DISTRIBUTION/AVAILABILITY STATEMENT

Distribution Statement A: Approved for Public Release, Distribution Unlimited

13. SUPPLEMENTARY NOTES

Accepted for publication in: The Journal of the Acoustical Society of America.

14. ABSTRACT

While Biot theory can successfully account for the dispersion observed in sand sediments, the attenuation at high frequencies has been observed to increase more rapidly than Biot theory would predict. In an effort to account for this additional loss, perturbation theory is applied to Biot's poroelastic equations to model the loss due to the scattering of energy from heterogeneities in the sediment. A general theory for propagation loss is developed and applied to a medium with a randomly varying frame bulk modulus. The theory predicts that these heterogeneities produce an overall softening of the medium as well as scattering of energy from the mean fast compressional wave into incoherent fast and slow compressional waves. This theory is applied to two poroelastic media: a weakly consolidated sand sediment and a consolidated sintered glass bead pack. The random variations in the frame modulus do not have significant effects on the propagation through the sand sediment but do play an important role in the propagation through the consolidated medium.

15. SUBJECT TERMS

Biot theory, propagation loss, poroelastic media, energy scattering, high frequency

16. SECURITY CLASSIFICATION OF:			17. LIMITATION OF ABSTRACT	18. NUMBER OF PAGES	19a. NAME OF RESPONSIBLE PERSON
a. REPORT	b. ABSTRACT	c. THIS PAGE			Brian Todd Hefner
U	U	U	U	39	19b. TELEPHONE NUMBER *(Include area code)* (206) 616-7558

Reset

Standard Form 298 (Rev. 8/98)
Prescribed by ANSI Std. Z39.18

Abstract

While Biot theory can successfully account for the dispersion observed in sand sediments, the attenuation at high frequencies has been observed to increase more rapidly than Biot theory would predict. In an effort to account for this additional loss, perturbation theory is applied to Biot's poroelastic equations to model the loss due to the scattering of energy from heterogeneities in the sediment. A general theory for propagation loss is developed and applied to a medium with a randomly varying frame bulk modulus. The theory predicts that these heterogeneities produce an overall softening of the medium as well as scattering of energy from the mean fast compressional wave into incoherent fast and slow compressional waves. This theory is applied to two poroelastic media: a weakly consolidated sand sediment and a consolidated sintered glass bead pack. The random variations in the frame modulus do not have significant effects on the propagation through the sand sediment but do play an important role in the propagation through the consolidated medium.

PACS numbers: 43.30.Ma, 43.20.Gp, 43.20.Jr

I. INTRODUCTION

For sand sediments there has been a long-running debate about the physical mechanisms by which sound is attenuated as it passes through the sediment. This debate has typically centered on two explanations: that the loss is due to viscous flow through the pores formed by the sand grains which compose the sediment or that the loss is due to the interactions between the sand grains at the grain contacts. The first of these mechanisms was applied by Stoll[1] using the theory for fluid-saturated poroelastic solids developed by Biot[2,3]. This theory predicts that for low frequencies, the attenuation will increase as the square of the frequency while at higher frequencies it will increase as the square root of the frequency. The theory also suggests that the change in attenuation is accompanied by an increase in sound speed. The grain contact theory was proposed by Hamilton[4] and later revisited by Buckingham[5]. This theory predicts that the attenuation is linear in frequency over all frequencies while the sound speed exhibits little or no dispersion.

A number of experiments have been performed in both laboratory and ocean sediments to test the predictions of these theories. Hamilton collected a number of the measurements and found that, in the aggregate, the attenuation is linear in frequency[4]. This observation has been supported by the relatively recent sediment acoustic experiments in 1999 and 2004 (SAX99 and SAX04 respectively) for high frequencies[6] as well as recent laboratory experiments examining propagation through glass bead sediments[7]. In the laboratory experiments, while Biot theory was unable to capture the frequency dependence of the attenuation, it did predict the overall scaling of the attenuation as the viscosity of the pore fluid was increased. Also the sound speeds measured during SAX99 and SAX04 both exhibit dispersion that for the mid- to high-frequencies is consistent with the predictions of Biot theory. For low frequencies, there remains some uncertainty as to both the asymptotic value for the sound speed as the frequency goes to zero and the frequency dependence of the attenuation[6]. Measurements in ocean sediments have shown that for low frequencies the attenuation is proportional to f^n, where f is the frequency and n varies from 1.5 to 2.0[8].

These measurements have led to attempts to create modifications to each theory to capture aspects of the other. Buckingham's grain-to-grain shearing model was recently modified to incorporate a linear loss mechanism at the grain contacts in addition to the original strain-hardening mechanism[9]. This produces a linear frequency dependance for the attenuation at high-frequencies and a dependence similar to Biot theory in the mid- to low-frequencies. Likewise, several researchers have proposed a linear loss mechanism at the grain contacts which would manifest as complex, frequency-dependent frame moduli in Biot theory thus creating a hybrid of the two approaches[7,10].

In this paper, we develop an alternative theory which treats the sediment as a poroelastic medium using Biot theory but incorporates losses due to scattering from heterogeneities in the structure of the sand sediment. These heterogeneities can exist in any of the parameters on which Biot theory depends such as the porosity or permeability. For a fast compressional wave propagating through the sediment, energy will be scattered from the coherent wave into incoherent fast compressional waves when the wavelength of the wave is on order of the size of the heterogeneity. For variations on the order of a few grains, these losses will occur at much higher frequencies than has been observed in the experiments discussed above. However, both the slow compressional wave and the shear wave are considerably slower than the fast wave and consequently have shorter wavelengths. When these wavelengths are on the order of the heterogeneities, mode conversion can occur scattering energy from the fast compressional wave into incoherent slow or shear waves leading to additional attenuation.

This type of attenuation mechanism has been explored in the context of seismic propagation by a number of researchers. Pride and Berryman have developed a model for the special case of a "double porosity" material such as a mixture of sand and clay where the heterogeneity has a single, dominant length scale[11,12]. Pride and Masson conducted a series of numerical simulations to measure the compressibility of a heterogenous poroelastic material which has a self-affine fractal structure[13,14]. They found that the frequency dependence of the attenuation is a function of the Hurst exponent which characterizes the fractal heterogeneity. Muller and Gurevich[15,16] used statistical smoothing of the Biot Green's tensor to

model propagation through a heterogenous Biot medium for frequencies below the critical Biot frequency,

$$\omega \ll \omega_B = \frac{\beta\eta}{\kappa\rho_f} \tag{1}$$

where $\omega = 2\pi f$, β is the porosity, η is the viscosity of the pore fluid, ρ_f is the density of the pore fluid, and κ is permeability. In this paper, we use perturbation theory to develop a poroelastic wave equation which contains the first-order scattering effects that can be applied to heterogenous media above and below the critical frequency. The perturbation technique used was first developed by Karal and Keller to examine scalar, elastic, and electromagnetic propagation through random media[17].

Evidence for the existence of heterogeneities in sand sediments can be found in recent work in the physics of granular materials. Experiments[18] and simulations[19] have shown that the complexity of a random packing of sand grains or beads leads to the formation of force networks or "chains" where a small subset of the grains will carry a majority of any load applied to the medium as well as the overburden pressure of the grains themselves. Hertz-Mindlin theory relates the forces at the grain contacts to the frame moduli of the medium[20] and one would expect that in applying that theory, these force chains should manifest as small scale heterogeneities in frame moduli. Likewise, recent analysis of simulations of random packings of spheres[21] as well as measurements on sand sediments[22] indicate that the porosity should also exhibit random spatial variations. In this paper, we will only consider variations in the frame bulk modulus to simplify the development of the theoretical framework which will be used to consider variations in the porosity in a subsequent paper.

Note that while there has been some debate over whether or not the Biot slow wave can be observed in a sand sediment[23–25], the theory presented here is not predicated on the existence of a propagating Biot slow wave. For small values of the frame moduli, Biot theory predicts that the Biot slow wave should be highly attenuated making it difficult if not impossible to observe[26]. However, it should still be possible to scatter energy into this type of wave, in which case, that energy will be quickly converted into heat.

In Section II, we begin by expressing the heterogenous poroelastic equations in a form

to which we can apply perturbation theory, the details of which are developed in Section III. The general properties of the resulting perturbed wave equation including the limits of applicability and causality are examined in Section IV. In Section V, the perturbation theory is applied to the SAX99 and sintered glass bead sediments and the results are discussed in Section VI.

II. HETEROGENOUS BIOT'S POROELASTIC EQUATIONS

If the frame moduli and the porosity are allowed to vary as functions of position within a poroelastic medium, Biot's poroelastic equations can be expressed as[27]

$$\begin{aligned} &\partial_i[(H-2\mu_b)\,\nabla\cdot\mathbf{u}-C\nabla\cdot\mathbf{w}]+ \\ &\quad\partial_j\left[\mu_b\left(\partial_i u_j+\partial_j u_i\right)\right]=-\omega^2\rho u_i+\omega^2\rho_f w_i \end{aligned} \tag{2}$$

and

$$\partial_i\left[C\nabla\cdot\mathbf{u}-M\nabla\cdot\mathbf{w}\right]=-\omega^2\rho_f u_i+\omega^2\rho^* w_i, \tag{3}$$

where μ_b is the shear modulus of the sediment frame, $\mathbf{u}$ is the displacement field of the frame, $\mathbf{w}=\beta\left(\mathbf{u}-\mathbf{u_f}\right)$ is the relative displacement of the pore fluid to the frame, $\mathbf{u_f}$ is the displacement field of the pore fluid, ρ_g is the sediment particle mass density, and

$$H=\frac{\left(K_g-K_b\right)^2}{D-K_b}+K_b+\frac{4\mu_b}{3}, \tag{4}$$

$$C=\frac{K_g\left(K_g-K_b\right)}{D-K_b}, \tag{5}$$

$$M=\frac{K_g^2}{D-K_b}, \tag{6}$$

$$D=K_g\left[1+\beta\left(\frac{K_g}{K_f}-1\right)\right], \tag{7}$$

$$\rho=\left(1-\beta\right)\rho_g+\beta\rho_f, \tag{8}$$

and

$$\rho^*=\frac{\alpha\rho_f}{\beta}+\frac{iF\eta}{\kappa\omega}, \tag{9}$$

where K_g is the bulk modulus of the individual grains, K_b is the bulk modulus of the sediment frame, K_f is the bulk modulus of the pore fluid, α is the tortuosity, and the parameter F represents the deviation from Poiseuille flow as frequency increases. The expression for F is given and discussed in Ref.28.

The two equations can be consolidated into a single, matrix equation as

$$\begin{aligned}\nabla\left[\left(\left[\mathsf{K}\right]-2\left[\tilde{\mu}\right]\right)\nabla\cdot\mathbf{U}\right]+\nabla\times\left(\left[\tilde{\mu}\right]\nabla\times\mathbf{U}\right)+\\ 2\left[\tilde{\mu}\right]\nabla^2\mathbf{U}+2\left(\nabla\left[\tilde{\mu}\right]\cdot\nabla\right)\mathbf{U}+\\ \left[\rho\right]\omega^2\mathbf{U}=0\end{aligned} \tag{10}$$

where

$$\left[\mathsf{K}\right]=\begin{bmatrix}H & -C\\ C & -M\end{bmatrix}, \tag{11}$$

$$\left[\rho\right]=\begin{bmatrix}\rho & -\rho_f\\ \rho_f & -\rho^*\end{bmatrix}, \tag{12}$$

$$\left[\tilde{\mu}\right]=\begin{bmatrix}\mu_b & 0\\ 0 & 0\end{bmatrix}, \tag{13}$$

and

$$\mathbf{U}=\begin{bmatrix}\mathbf{u}\\ \mathbf{w}\end{bmatrix}. \tag{14}$$

which for the homogenous case, when $[\mathsf{K}]=[\mathsf{K}_0]$ and $[\tilde{\mu}]=[\tilde{\mu}_0]$ are constants, reduces to

$$\left(\left[\mathsf{K}_0\right]-\left[\tilde{\mu}_0\right]\right)\nabla\left(\nabla\cdot\mathbf{U}\right)+\left[\tilde{\mu}_0\right]\nabla^2\mathbf{U}+\left[\rho_0\right]\omega^2\mathbf{U}=0. \tag{15}$$

The homogenous equation can be solved in terms of potentials to obtain the fast and slow compressional wavenumbers and the shear wavenumber.

In the following, we are going to look at heterogeneities due to the frame bulk modulus only. For this case, the frame shear modulus and the porosity are constant and the poroelastic equation becomes

$$\nabla\left(\left[\mathsf{K}\right]\nabla\cdot\mathbf{U}\right)-\left[\tilde{\mu}_0\right]\nabla\times\left(\nabla\times\mathbf{U}\right)+\left[\rho_0\right]\omega^2\mathbf{U}=0. \tag{16}$$

III. PERTURBATION THEORY

In this paper we consider a poroelastic medium in which the frame bulk modulus varies randomly with position,

$$K_b(\mathbf{r}) = K_{b0} + \delta K_b(\mathbf{r}), \tag{17}$$

where $K_{b0} = \langle K_b(\mathbf{r}) \rangle$ is the average over an ensemble of realizations of the medium (denoted by $\langle \cdot \rangle$), $\delta K_b(\mathbf{r})$ is the local fluctuation of the bulk modulus, and $\langle \delta K_b(\mathbf{r}) \rangle = 0$. The bulk modulus enters the heterogenous poroelastic equations through the Biot coefficients in the matrix $[\mathsf{K}]$. To account for the random variations, we will expand this matrix as a Taylor series about the mean value,

$$[\mathsf{K}] = [\mathsf{K}_0] + [\mathsf{F}_{\mathsf{b1}}]\,\delta K_b + \frac{1}{2}[\mathsf{F}_{\mathsf{b2}}]\,\delta K_b^2 + \ldots, \tag{18}$$

where

$$[\mathsf{F}_{\mathsf{bn}}] = \frac{\partial^n [\mathsf{K}_0]}{\partial K_b^n}. \tag{19}$$

This expansion can now be substituted into the poroelastic equation given by Eq. (16). If the heterogenous poroelastic equation is rewritten as

$$\mathfrak{L}([\mathsf{K}]) \cdot \mathbf{U} = 0, \tag{20}$$

substitution of the expanded expressions yields,

$$(\mathfrak{L}_0 + \mathfrak{L}_1 + \mathfrak{L}_2 + \ldots) \cdot \mathbf{U} = 0, \tag{21}$$

where $\mathfrak{L}_0 \cdot \mathbf{U} = 0$ is the homogenous poroelastic equation given by Eq. (15). We will also expand the displacement, $\mathbf{U}$, as

$$\mathbf{U} = \langle \mathbf{U} \rangle + \mathbf{U_s}, \tag{22}$$

where $\langle \mathbf{U} \rangle$ is the mean coherent field and $\mathbf{U_s}$ is the incoherent, scattered field for which $\langle \mathbf{U_s} \rangle = 0$. Substitution of Eq. (22) into Eq. (21) yields,

$$\mathfrak{L}_0 \cdot \langle \mathbf{U} \rangle + \mathfrak{L}_0 \cdot \mathbf{U_s} + \mathfrak{L}_1 \cdot \langle \mathbf{U} \rangle + \mathfrak{L}_1 \cdot \mathbf{U_s} + \mathfrak{L}_2 \cdot \langle \mathbf{U} \rangle = 0, \tag{23}$$

where we have neglected all terms higher than second order.

Our goal is to obtain a solution for the coherent field, $\langle \mathbf{U} \rangle$. Since $\langle \mathfrak{L}_1 \rangle = 0$, the mean of Eq. (23) yields

$$\mathfrak{L}_0 \cdot \langle \mathbf{U} \rangle + \langle \mathfrak{L}_1 \cdot \mathbf{U_s} \rangle + \langle \mathfrak{L}_2 \rangle \cdot \langle \mathbf{U} \rangle = 0. \tag{24}$$

Subtracting Eq. (24) from Eq. (23) and neglecting all terms higher than first order, we find the equation for $\mathbf{U_s}$ in terms of $\langle \mathbf{U} \rangle$,

$$\mathfrak{L}_0 \cdot \mathbf{U_s} = -\mathfrak{L}_1 \cdot \langle \mathbf{U} \rangle . \tag{25}$$

This equation can be solved using the poroelastic Green's tensor, which is a solution to (see Appendix A)

$$\mathfrak{L}(\mathbf{r}) \cdot \mathfrak{G}(\mathbf{r}, \mathbf{r}') = -\delta(\mathbf{r}, \mathbf{r}') [\mathrm{I}] \mathfrak{I}, \tag{26}$$

to yield the solution for $\mathbf{U_s}$,

$$\mathbf{U_s}(\mathbf{r}) = \int \mathfrak{G}(\mathbf{r}, \mathbf{r}') \cdot \mathfrak{L}_1(\mathbf{r}') \cdot \langle \mathbf{U}(\mathbf{r}') \rangle \, d^3\mathbf{r}'. \tag{27}$$

Substituting this expression back into Eq. (24), we find the final equation for a poroelastic wave propagating through a heterogenous medium,

$$\begin{aligned} &\mathfrak{L}_0(\mathbf{r}) \cdot \langle \mathbf{U} \rangle (\mathbf{r}) \\ &\quad + \left\langle \mathfrak{L}_1(\mathbf{r}) \cdot \int \mathfrak{G}(\mathbf{r}, \mathbf{r}') \cdot \mathfrak{L}_1(\mathbf{r}') \cdot \langle \mathbf{U}(\mathbf{r}') \rangle \, d^3\mathbf{r}' \right\rangle \\ &\quad + \langle \mathfrak{L}_2(\mathbf{r}) \rangle \cdot \langle \mathbf{U}(\mathbf{r}) \rangle = 0. \end{aligned} \tag{28}$$

This result is identical to Karal and Keller's Eq. (14) in Ref. 17. for the general case of scalar, elastic, or electromagnetic wave propagation in a random medium.

In order to apply Eq. (28) to the case of poroelastic waves propagating through a heterogenous medium, we begin by substituting Eq. (18) into the heterogenous poroelastic equation, Eq. (16). The result can be separated into three parts: $\mathfrak{L}_0 \cdot \mathbf{U}$, which is identical to Eq. (16) with the replacement of $[\mathsf{K}]$ by $[\mathsf{K}_0]$,

$$\mathfrak{L}_1 \cdot \mathbf{U} = [\mathsf{F_{b1}}] \nabla (\delta K_b \nabla \cdot \mathbf{U}) \tag{29}$$

and

$$\mathfrak{L}_2 \cdot \mathbf{U} = \frac{1}{2} \left[\mathsf{F}_{\mathsf{b2}}\right] \nabla \left(\delta K_b^2 \nabla \cdot \mathbf{U}\right). \tag{30}$$

The last term in Eq. (28) can be determined by substituting $\mathbf{U} = \langle \mathbf{U} \rangle$ in Eq. (30) and taking the mean of the result. Since $\langle \delta K_b \rangle = 0$, this yields,

$$\langle \mathfrak{L}_2 (\mathbf{r}) \rangle \cdot \langle \mathbf{U} \rangle = \frac{1}{2} \left[\mathsf{F}_{\mathsf{b2}}\right] \sigma_{bb}^2 \nabla \left(\nabla \cdot \langle \mathbf{U} \rangle\right), \tag{31}$$

where $\sigma_{bb}^2 = \langle \delta K_b^2 \rangle$ is the variance of the perturbation in the frame bulk modulus.

Consider the integral factor in Eq. (28) involving the Green's tensor. This factor can be viewed as the field due to a source $\mathfrak{L}_1 \cdot \mathbf{U}$. Eq. (29) shows that this source is the gradient of a scalar field, from which Eq. (A15) leads to

$$\begin{aligned} &\int \mathfrak{G} (\mathbf{r}, \mathbf{r}') \cdot \mathfrak{L}_1 (\mathbf{r}') \cdot \langle \mathbf{U} (\mathbf{r}') \rangle \, d^3 \mathbf{r}' \\ &= \sum_{n=1}^{2} \left[\mathsf{G}_n\right] \left[\mathsf{F}_{\mathsf{b1}}\right] k_n^2 \nabla \int g_n (R) \, \delta K_b (\mathbf{r}') \, \nabla' \cdot \langle \mathbf{U} (\mathbf{r}') \rangle \, d^3 \mathbf{r}'. \end{aligned} \tag{32}$$

where ∇' denotes differentiation with respect to $\mathbf{r}'$ and the $g_n (R)$ are defined in Appendix A. Note that as a consequence of the source being the gradient of a scalar field, there is no mode scattering into shear waves. Operating on this expression with $\mathfrak{L}_1$ and taking the mean will yield the second term in Eq. (28),

$$\begin{aligned} &\left\langle \mathfrak{L}_1 (\mathbf{r}) \cdot \int \mathfrak{G} (\mathbf{r}, \mathbf{r}') \cdot \mathfrak{L}_1 (\mathbf{r}') \cdot \langle \mathbf{U} (\mathbf{r}') \rangle \, d^3 \mathbf{r}' \right\rangle = \\ &- \left[\mathsf{F}_{\mathsf{b1}}\right] \sum_{n=1}^{2} \left[\mathsf{G}_n\right] \left[\mathsf{F}_{\mathsf{b1}}\right] k_n^2 \times \\ &\left\{ k_n^2 \nabla \left\langle \delta K_b (\mathbf{r}) \int g_n (R) \, \delta K_b (\mathbf{r}') \, \nabla' \cdot \langle \mathbf{U} (\mathbf{r}') \rangle \, d^3 \mathbf{r}' \right\rangle \right. \\ &\left. + \sigma_{bb}^2 \nabla \left(\nabla \cdot \langle \mathbf{U} (\mathbf{r}) \rangle\right) \right\} \end{aligned} \tag{33}$$

where we have used,

$$\nabla^2 g_n (R) = -k_n^2 g_n (R) - \delta (R). \tag{34}$$

In Eq. (33), the mean is taken only over the product of the frame modulus variations and the resulting expression is the covariance of the modulus variations, $C_{bb} (\mathbf{r}, \mathbf{r}') =$

$\langle \delta K_b(\mathbf{r})\, \delta K_b(\mathbf{r}') \rangle$. If we assume that the variations in the modulus are statistically homogenous (spatially stationary) and isotropic, then the covariance should depend only on the distance $R = |\mathbf{r} - \mathbf{r}'|$ and $C_{bb}(\mathbf{r}, \mathbf{r}') = C_{bb}(R)$.

In order to solve the perturbation equation, we will assume a plane solution given by

$$\langle \mathbf{U}(\mathbf{r}) \rangle = \mathbf{A} e^{i\mathbf{k}\cdot\mathbf{r}}. \tag{35}$$

With this expression for the mean field and using Eqs. (15), (31), and (33), Eq. (16) becomes

$$\begin{aligned}
&-([\mathsf{K}_0] - [\tilde{\mu}_0])\,\mathbf{k}\,(\mathbf{k}\cdot\mathbf{A}) - k^2\,[\tilde{\mu}_0]\,\mathbf{A} + [\rho_0]\,\omega^2\mathbf{A} \\
&+[\mathsf{F_{b1}}] \sum_{n=1}^{2} [\mathsf{G}_n]\,[\mathsf{F_{b1}}]\,k_n^2 \mathbf{k}\,(\mathbf{k}\cdot\mathbf{A}) \times \\
&\int \left(k_n^2 g_n(R) + \delta(R)\right) C_{bb}(R)\, e^{-i\mathbf{k}\cdot\mathbf{R}} d^3\mathbf{R} \\
&-\frac{1}{2}\,[\mathsf{F_{b2}}]\,\sigma_{bb}^2 \mathbf{k}\,(\mathbf{k}\cdot\mathbf{A}) = 0,
\end{aligned} \tag{36}$$

where we have substituted $\mathbf{R} = \mathbf{r} - \mathbf{r}'$ and integrated with respect to $\mathbf{R}$. Evaluating the integral of the delta function and using the relation given in Eq. (A16), we can rearrange the terms to express the wave equation in the much simpler form,

$$-([\mathsf{K_{eff}}] - [\tilde{\mu}_0])\,\mathbf{k}\,(\mathbf{k}\cdot\mathbf{A}) - k^2\,[\tilde{\mu}_0]\,\mathbf{A} + [\rho_0]\,\omega^2\mathbf{A} = 0, \tag{37}$$

where the effects of the bulk frame modulus variations on the wave propagation have been folded into the effective Biot coefficient matrix,

$$\begin{aligned}
[\mathsf{K_{eff}}] = [\mathsf{K}_0] &\\
&- [\mathsf{F_{b1}}] \sum_{n=1}^{2} [\mathsf{G}_n]\,[\mathsf{F_{b1}}]\,k_n^4 I_n \\
&- \left([\mathsf{F_{b1}}]\,[\mathsf{K}_0]^{-1}\,[\mathsf{F_{b1}}] - \frac{1}{2}\,[\mathsf{F_{b2}}]\right)\sigma_{bb}^2
\end{aligned} \tag{38}$$

where

$$I_n = \int g_n(R)\, C_{bb}(R)\, e^{-i\mathbf{k}\cdot\mathbf{R}} d^3\mathbf{R}. \tag{39}$$

When the variance of the modulus variations goes to zero, the effective matrix reduces to $[\mathsf{K}_0]$ as one would expect. The second term which contains the integration over the covariance will lead to dispersion and an increase in attenuation as a function of frequency as will be seen in the examples shown in Section V. The last term in this expression does not depend on the form of the covariance nor does it have any frequency dependence. This term represents the softening of the medium due to the variations in the frame modulus which is discussed in more detail in the next section and in Appendix B.

The result in Eq. (37) has three solutions: a shear wave, a slow compressional wave, and a fast compressional wave. For the shear wave, the displacement of the wave is perpendicular to the wave vector, $\mathbf{k}$, and $\mathbf{k}\left(\mathbf{k}\cdot\mathbf{A}\right)=0$. The random variations in the bulk frame modulus have no effect on the shear wave and the resulting expression,

$$-k^2\left[\tilde{\mu}_0\right]\mathbf{A}+\left[\rho_0\right]\omega^2\mathbf{A}=0, \tag{40}$$

is identical to the result for the shear wave in a homogenous medium. For the compressional waves, the displacement is parallel to the wave vector and Eq. (37) reduces to

$$-\left[\mathsf{K}_{\mathsf{eff}}\right]k^2\mathbf{A}+\left[\rho_0\right]\omega^2\mathbf{A}=0, \tag{41}$$

which has two solutions since it is a 2×2 matrix equation (Note that the equation for the shear wave has only a single solution since only the first element in $[\tilde{\mu}_0]$ is non-zero). For the remainder of this paper, we will focus on the fast compressional wave solution, k_1.

The integral in $[\mathsf{K}_{\mathsf{eff}}]$ given by Eq. (39) can be partially solved by separating it into its radial and surface components,

$$I_n=\int g_n\left(R\right)C_{bb}\left(R\right)\int e^{-i\mathbf{k}\cdot\mathbf{R}}dSdR. \tag{42}$$

The integration with respect to dS can be performed yielding,

$$\int e^{-i\mathbf{k}\cdot\mathbf{R}}dS=\frac{4\pi R}{k}\sin kR. \tag{43}$$

Substituting this result back into Eq. (42) and substituting the expression in Eq. (A7) for the scalar green's function, $g_n\left(R\right)$, the final integral becomes,

$$I_n=\frac{1}{k}\int_0^\infty \mathrm{e}^{ik_nR}C_{bb}\left(R\right)\sin\left(kR\right)dR. \tag{44}$$

The fast compressional wave propagating through a poroelastic medium with a randomly varying bulk frame modulus can now be determined from Eq. (41) where $[\mathsf{K}_{\mathsf{eff}}]$ is given by Eq. (38) and I_n is given by Eq. (44).

In the low frequency limit, when ω satisfies Eq. (1), the effective wavenumber determined from Eq. (41) has a much simpler form. In this limit, $\rho^* \to i\eta/\kappa\omega$, and the unperturbed compressional wavenumbers become

$$k_1 = \omega\sqrt{\frac{\rho}{H}} \quad \text{and} \quad k_2 = \omega\sqrt{\frac{\rho^*}{N}}, \tag{45}$$

where $N = M - C^2/H$ and k_1 is real. The slow wave, k_2, in this low frequency limit, is a solution to a diffusion equation (See Eq. (5a) and (5b) in Ref. 26.) In this limit, if we consider only scattering from fast into slow waves and assume that the compressional wavenumbers satisfy

$$\frac{|k_1|}{|k_2|} \ll 1, \tag{46}$$

then the effective fast compressional wavenumber reduces to

$$k_{eff} = \omega\sqrt{\frac{\rho}{H_{eff}}}, \tag{47}$$

where

$$H_{eff} = H - \Delta_2\sigma_{bb}^2 - \Delta_1 k_2^2 \int_0^\infty C_{bb}(R)\, \mathrm{e}^{ik_n R} R dR, \tag{48}$$

$$\Delta_1 = 2C\frac{\partial H}{\partial K_b}\frac{\partial C}{\partial K_b} - M\left(\frac{\partial H}{\partial K_b}\right)^2 - H\left(\frac{\partial C}{\partial K_b}\right)^2, \tag{49}$$

and

$$\Delta_2 = \Delta_1 - \frac{1}{2}\frac{\partial^2 H}{\partial K_b^2}. \tag{50}$$

This result is equivalent to the effective wavenumber in Eqs. (49), (50), and (51) of Ref. 16 by Müller and Gurevich when there are no variations in the shear modulus.

IV. GENERAL PROPERTIES OF COMPRESSIONAL SOUND SPEED AND ATTENUATION

We will explore the behavior of the perturbed fast compressional wave for two types of media: the SAX99 sand sediment and a water-saturated sintered glass bead pack. The

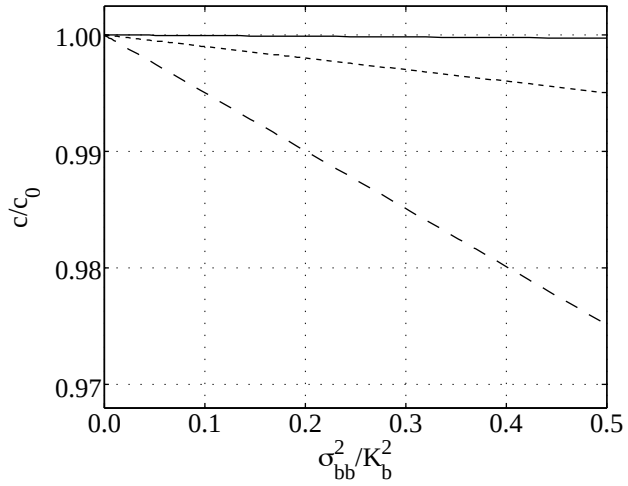

(a)

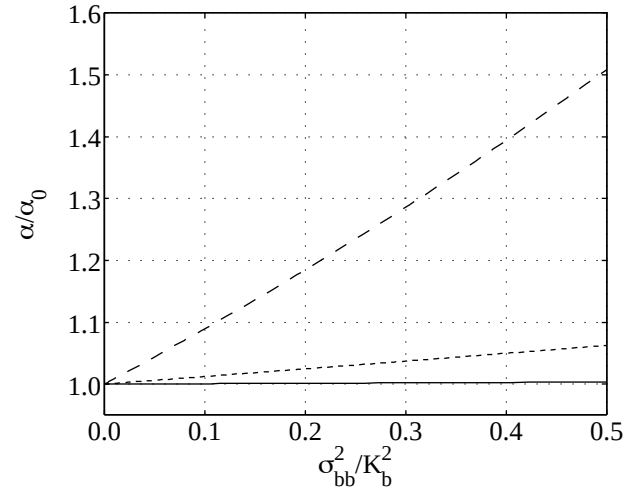

(b)

FIG. 1. (a) Fast compressional sound speed and (b) attenuation determined from Eq. (41) with $[\mathsf{K}_{\mathsf{eff}}]$ given by Eq. (54) as a function of the variance, σ_{bb}^2, of the moduli variations normalized by K_{b0}^2. Both the sound speed and the attenuation have been normalized by their respective values when $\sigma_{bb} = 0$. These results were calculated for $f = 1$ kHz using the SAX99 sediment parameters in Table I while the value of the mean bulk modulus was increased from 4.36×10^7 Pa for the solid line, to 4.36×10^8 Pa for the short dashed line, and to 2.18×10^9 Pa for the long dashed line.

SAX99 sediment is a well-characterized sand sediment which, like most sand sediments, has a small frame bulk modulus. The values for the SAX99 sediment given in Table I were taken from Table I of Ref. 6. The sintered bead pack was chosen since it has a much larger frame bulk modulus and has been studied extensively as a poroelastic medium[26,29,30]. A majority of the material parameters for the sintered glass bead pack were taken from Sample 2 in Table III of Ref. 30 while the fluid parameters were chosen to correspond to the water parameters measured during SAX99. These two media allow us to understand the effects of scattering from heterogeneities for both a weak and a strong frame.

A. Softening of the poroelastic medium

In order to understand the behavior of the fast compressional wave in a heterogenous medium, we begin by considering the solution to the perturbed wave equation for a poroelastic medium where the bulk frame modulus variations are related by the exponential correlation function,

$$C_{bb}(R) = \sigma_{bb}^2 e^{-R/L} \tag{51}$$

where L is the characteristic length scale of the bulk modulus variations. The three-dimensional Fourier transform of this correlation function yields the commonly encountered power spectrum,

$$W_{bb}(k) = \frac{\sigma_{bb}^2}{\pi^2 L \left(k^2 + L^{-2}\right)^2}. \tag{52}$$

The integral given in Eq. (44) can be solved analytically for the exponential correlation function to yield,

$$I_n = \frac{\sigma_{bb}^2}{\left(L^{-1} - ik_n\right)^2 + k^2}. \tag{53}$$

In the following section, we will explore this result in detail, but here we will consider the limiting case as $L \to 0$. This corresponds to a poroelastic medium in which the frame modulus is completely random between any two points in the medium. In this case, $I_n = 0$

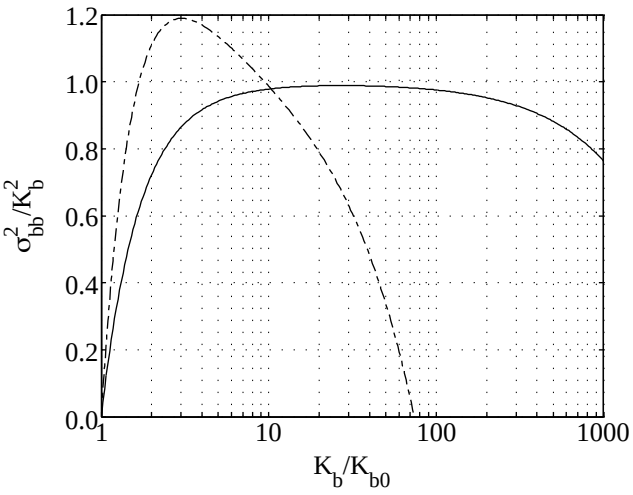

FIG. 2. Values of σ_{bb}^2/K_b^2 for which $[\mathsf{K_{eff}}]$ remains equal to $[\mathsf{K}_0]$ for the SAX99 sediment parameters (solid line) and the sintered glass bead parameters (dash-dot line) as K_b is increased by three orders of magnitude.

and the effective Biot coefficient matrix reduces to

$$[\mathsf{K_{eff}}] = [\mathsf{K}_0] - \left([\mathsf{F_{b1}}] [\mathsf{K}_0]^{-1} [\mathsf{F_{b1}}] - \frac{1}{2} [\mathsf{F_{b2}}] \right) \sigma_{bb}^2. \tag{54}$$

As shown in Appendix B, this expression for $[\mathsf{K_{eff}}]$ is the effective response of a poroelastic medium with a heterogenous frame modulus under static compression. The elastic response of the medium is dominated by the weaker elements of the frame and consequently the heterogenous frame is softer than the homogenous medium.

This softening has two important consequences. First it produces a decrease in the sound speed that is proportional to the variance as seen in Figure 1(a). The sound speed has been calculated using the SAX99 sediment parameters given in Table I for the solid line. The bulk frame modulus was increased by an order of magnitude for the short-dashed line and two orders of magnitude for the long-dashed line. This softening of the medium also leads to an increase in the attenuation as the variance increases. The attenuation which corresponds to the sound speed plotted in Figure 1(a) is shown in Figure 1(b).

This dependence on the variance for both the sound speed and attenuation may have an important influence on the choice of frame modulus used in Biot calculations. For a static

measurement of the elastic response of a sediment, if the frame modulus is heterogenous, the value determined for the bulk frame modulus will not be the mean frame modulus but instead a smaller value. Likewise for a measurement of the sound speed, the frame modulus determined from a best fit of the data would again underestimate the mean value for the frame modulus. If K_{b0} is the mean bulk modulus for a homogenous sediment, it is possible to find values for σ_{bb}^2 and K_b that satisfy,

$$[\mathsf{K}_{\mathsf{eff}}]\left(K_b, \sigma_{bb}^2\right) = [\mathsf{K}_0]\left(K_{b0}, 0\right), \tag{55}$$

where the effective Biot coefficients as a function of σ_{bb}^2 are equal to the coefficients when $\sigma_{bb}^2 = 0$. This equation can be solved for σ_{bb}^2,

$$\sigma_{bb}^2 = \frac{(D - K_b)\left(K_b - K_{b0}\right)}{(D - K_{b0})}\left(K_b + \frac{4\mu_b}{3}\right). \tag{56}$$

This result is plotted in Figure 2 for both the SAX99 and sintered glass bead sediments. For the SAX99 sediment, as the bulk modulus is increased, the normalized variance comes very close to unity and then decreases while for the sintered glass beads, the normalized variances increases to almost 1.2 before decreasing to zero. The variance becomes zero when $K_b = D$, where D is given in Eq. (7). At this point H, C, and M diverge and both the perturbed and unperturbed wavenumbers equal zero.

For both media, Eq. (56) predicts that it is possible to choose values of σ_{bb}^2 and K_b where σ_{bb}^2 is almost equal to or, for the case of the sintered glass beads, larger than K_b^2. It is worth considering at this point whether or not large values could be realistic for actual sediments or other poroelastic media. The frame moduli are constrained to be positive by the nonnegative character of the strain energy for the medium[3]. If the probability distribution for the modulus variations is approximately Gaussian, a standard deviation, σ_{bb}, on the order of the mean value for the frame modulus would imply that at some locations within the medium, the local frame modulus would have to be negative, which would violate the constraint of the strain energy. However, the distribution of contact forces within real and simulated granular materials have been found to be approximately exponential. The

probability distribution for the frame modulus variations may exhibit a similar kind of distribution, in which case, the values for σ_{bb}^2 in Fig. 2 may be reasonable.

B. Limits of applicability

These large values for the variance also bring into question the validity of the assumptions behind the derivation in Section III, specifically whether it is sufficient to account for only the second-order scattering contributions to the mean propagating field. As the variance increases, it may be necessary to incorporate the effects of fourth order contributions. This can be done formally by retaining the fourth order terms in Eq. (23) and following the same procedure used in Eq. (24)-(28). While it may be possible to solve the resulting expression, the contributions of these higher order terms can be estimated in a more straightforward way to yield a necessary condition which must be met for the second order theory to be valid.

The second approach to testing the validity of the second order approximation follows the approaches of Rytov[31] and Müller[15]. They examine the next approximation for the kernel of mass operator, which replaces the unperturbed Green's function with the Green's function they obtained from the original approximation. For the current theory, it can be shown that an infinite subset of terms in the full expansion corresponding to Eq. (23) can be solved by replacing the Green's tensor in Eq. (38) with the mean Green's tensor, $\bar{\mathfrak{G}}\left(\mathbf{r},\mathbf{r}'\right)$ for the heterogenous medium. The mean Green's tensor can be found by considering the inhomogenous poroelastic equation with a spatially varying frame modulus,

$$\nabla\left(\left[\mathsf{K}\right]\nabla\cdot\bar{\mathfrak{G}}\right)+\left[\tilde{\mu}_0\right]\nabla\times\left(\nabla\times\bar{\mathfrak{G}}\right)+ \\ \left[\rho_0\right]\omega^2\bar{\mathfrak{G}}=-\delta\left(R\right)[\mathsf{I}]\ \mathfrak{I}. \tag{57}$$

We showed in Section III that the homogenous wave equation for the mean field can be expressed in terms of the unperturbed wave equation with $[\mathsf{K}_0]$ replaced by $[\mathsf{K}_{\mathsf{eff}}]$. It follows that the inhomogenous wave equation can be approximated in the same way and $\bar{\mathfrak{G}}$ is a

solution to

$$[\mathsf{K}_{\mathsf{eff}}]\,\nabla\left(\nabla\cdot\bar{\mathfrak{G}}\right)+[\tilde{\mu}_0]\,\nabla\times\left(\nabla\times\bar{\mathfrak{G}}\right)+$$
$$[\rho_0]\,\omega^2\bar{\mathfrak{G}}=-\delta\,(R)[\mathsf{I}]\;\mathfrak{I}. \tag{58}$$

The mean Green's tensor therefore has the same form as the unperturbed Green's tensor given by Eq. (A3) with $[\mathsf{G}_1]$ and $[\mathsf{G}_2]$ replaced by

$$\left[\bar{\mathsf{G}}_1\right]=\frac{[\mathsf{K}_{\mathsf{eff}}]^{-1}-[\rho_0]^{-1}\,\omega^{-2}\bar{k}_2^2}{\bar{k}_1^2-\bar{k}_2^2}, \tag{59}$$

and

$$\left[\bar{\mathsf{G}}_2\right]=\frac{[\mathsf{K}_{\mathsf{eff}}]^{-1}-[\rho_0]^{-1}\,\omega^{-2}\bar{k}_1^2}{\bar{k}_2^2-\bar{k}_1^2}, \tag{60}$$

where $\bar{k}_1$ and $\bar{k}_2$ are the mean compressional wavenumbers determined from Eq. (41). The mean compressional wavenumbers also replace the unperturbed wavenumbers in Eq. (A7).

The next approximation for the fast compressional wave can be found by substituting $\bar{\mathfrak{G}}$ for $\mathfrak{G}$ in Eq. (28). The solution to the new equation proceeds as before to yield the new effective Biot coefficient matrix,

$$\begin{aligned}\left[\mathsf{K}_{\mathsf{eff}}^{(2)}\right]&=[\mathsf{K}_0]\\&-[\mathsf{F}_{\mathsf{b1}}]\sum_{n=1}^{2}\left[\bar{\mathsf{G}}_n\right][\mathsf{F}_{\mathsf{b1}}]\,\bar{k}_n^4 I_n\\&-\left([\mathsf{F}_{\mathsf{b1}}]\,[\mathsf{K}_{\mathsf{eff}}]^{-1}[\mathsf{F}_{\mathsf{b1}}]-\frac{1}{2}[\mathsf{F}_{\mathsf{b2}}]\right)\sigma_{bb}^2,\end{aligned} \tag{61}$$

which can be substituted into the compressional wave equation to get the new effective wavenumber, $\bar{k}_1^{(2)}$.

The condition which must be met is that the contribution of this higher correction to the wavenumber be small compared to the second order correction to the wavenumber, which can be expressed as

$$\frac{\left|\bar{k}_1^{(2)}-\bar{k}_1\right|}{\left|\bar{k}_1-k_1\right|}\ll 1. \tag{62}$$

This constraint is a necessary condition which must be met in order for the second-order approximation to apply to heterogenous poroelastic medium.

C. Causality

For the low-frequency limits of the mean compressional wavenumber, given by Eqs. (47)-(50), Müller and Gurevitch showed that this result satisfied a twice-subtracted dispersion relation and hence was causal[16]. For the general wavenumber result, which is applicable at all frequencies, we cannot show analytically that the complex wavenumber satisfies a dispersion relation. It is possible however to numerically integrate a twice-subtracted dispersion relation for the real and imaginary parts of the mean wavenumber on a case by case basis. If we define an index of refraction, $n(\omega) = c_0\bar{k}_1/\omega$, where c_0 is an arbitrarily chosen real sound speed, then the twice subtracted dispersion relation that must be evaluated becomes

$$\begin{aligned} n^R(\omega) = n_1^R \frac{(\omega^2-\omega_1^2)}{(\omega_2^2-\omega_1^2)} + n_2^R \frac{(\omega^2-\omega_2^2)}{(\omega_1^2-\omega_2^2)} + \\ \frac{2}{\pi}\left(\omega^2-\omega_1^2\right)\left(\omega^2-\omega_2^2\right) \times \\ \int_0^\infty \frac{n^I(\omega')\,\omega' d\omega'}{\left(\omega'^2-\omega_1^2\right)\left(\omega'^2-\omega_2^2\right)\left(\omega'^2-\omega^2\right)}, \end{aligned} \tag{63}$$

where $n = n^R + in^I$. The indices $n_1 = n(\omega_1)$ and $n_2 = n(\omega_2)$ are evaluated at the arbitrary frequencies ω_1 and ω_2. Choosing $c_0 = \omega_1/\bar{k}_1(\omega_1)$, this equation can be numerically evaluated.

For the examples given in the next section, the dispersion relation given above was found to be satisfied to within the numerical errors of the calculation. This does not prove that the perturbed wavenumber is causal in all cases, but rather provides a strong indication that the theory is causal.

V. SOUND SPEED AND ATTENUATION FOR SPECIFIC CORRELATION FUNCTIONS

In order to model a heterogeneous medium using the theory developed in Section III, the correlation function for the bulk modulus variations must be known or determined from a fit to existing data. In this section we consider two examples of correlation functions frequently used in acoustics and geophysics.

The first of the correlation functions to be considered is the exponential correlation

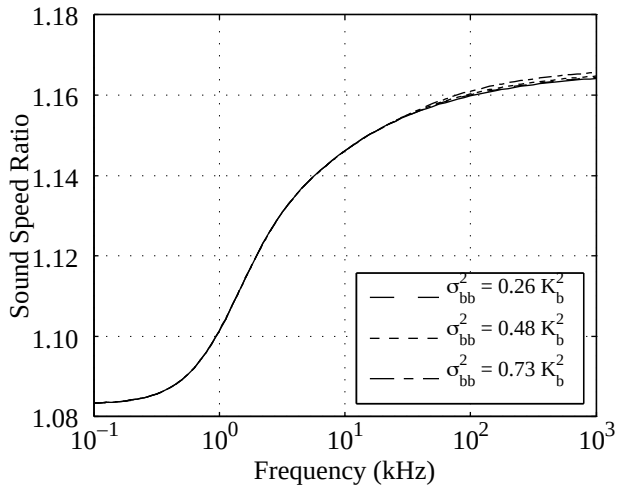

(a)

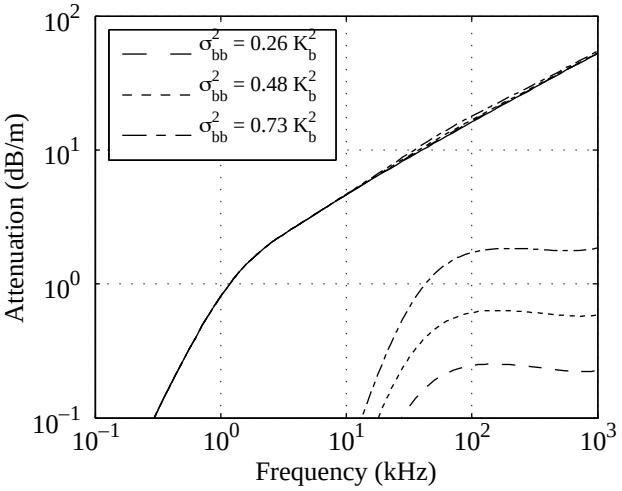

(b)

FIG. 3. Examples of (a) sound speed ratio and (b) attenuation for the SAX99 sediment assuming an exponential correlation for the frame bulk modulus variations. The correlation length is held fixed at $L = 1$ mm while the variance and the mean bulk modulus are increased. The variance is shown in the figures and the mean bulk modulus is $K_b = 1.18K_{b0}$ (long-dashed line), $K_b = 1.41K_{b0}$ (short-dashed line), and $K_b = 2.04K_{b0}$ (long-short dashed line). In (a) the sound speed ratio is defined as the sound speed of the sediment normalized by the sound speed of the pore fluid. In (b) the lower set of curves is the contribution of the scattering from the fast compressional waves into the slow compressional waves to the attenuation of the mean fast compressional wave. The solid line in each figure is the prediction of Biot theory with no variation in the bulk modulus and $K_b = K_{b0}$.

function which was introduced in the previous section. Using the solution of the integral for the exponential correlation given in Eq. (53), the effective Biot coefficient matrix becomes,

$$
\begin{aligned}
[\mathsf{K_{eff}}] = [\mathsf{K_0}] & \\
& - \sigma_{bb}^2 \left[\mathsf{F_{b1}}\right] \sum_{n=1}^{2} \left[\mathsf{G}_n\right] \left[\mathsf{F_{b1}}\right] \frac{k_n^4}{\left(L^{-1} - ik_n\right)^2 + k^2} \\
& - \sigma_{bb}^2 \left(\left[\mathsf{F_{b1}}\right] \left[\mathsf{K_0}\right]^{-1} \left[\mathsf{F_{b1}}\right] - \frac{1}{2} \left[\mathsf{F_{b2}}\right] \right).
\end{aligned} \tag{64}
$$

Note that the wavenumber that we seek to determine, k, appears in the denominator of the second term in $[\mathsf{K_{eff}}]$. In order to solve the wave equation, we approximate the wavenumber in the denominator by the unperturbed fast wavenumber, k_1. The validity of this approximation can be evaluated by substituting $\bar{k_1}$ into the denominator and iterating until the solution converges. For the examples given here, this approximation yields a solution that is not significantly different than the iterated solution.

Examples of the sound speed and attenuation evaluated using Eq. (64) as a function of σ_{bb}^2 are shown in Figure 3 for the SAX99 sediment. In each of these cases, the correlation length was held fixed at $L = 1$ mm and K_b was increased according to Eq. (56) to insure that the low frequency sound speed matches the unperturbed result. For the values of K_b and σ_{bb}^2 chosen, the sound speed and the attenuation are only weakly affected by the scattering from fast into slow compressional waves while the fast to fast wave scattering occurs at much higher frequencies. The magnitude of the scattering contribution to the attenuation can be seen in Fig. 3(b) where the set of curves in the lower right-hand corner of the figure were determined by subtracting the unperturbed attenuation from the perturbed result. Energy begins to scatter from the mean fast compressional wave into the slow wave when $k_2 L \approx 1$ and then the attenuation due to this mode conversion levels off at $k_2 L \approx 10$.

As noted in Fig. 2, it is possible to choose larger values for K_b and σ_{bb}^2 that satisfy the relation given in Eq. (56). However, if we evaluate the condition given in Eq. (62) which determines whether the second order scattering theory is sufficient to model the propagating field, we find that the right hand side of Eq. (62) is equal to 0.1, 0.25, and 0.65 for the three cases examined in the figure. We have, therefore, already begun to violate the inequality in

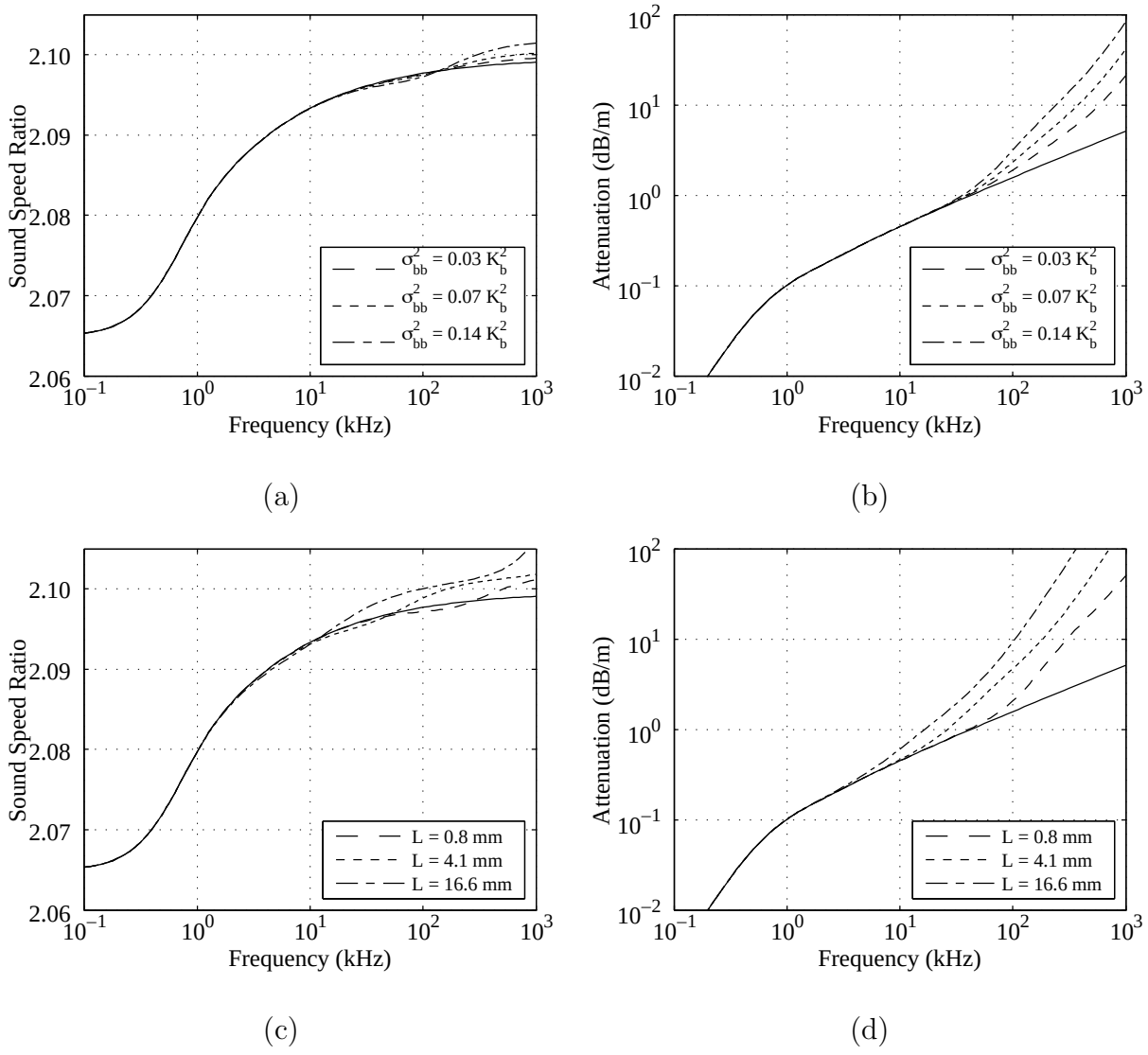

FIG. 4. Examples of sound speed ratio and attenuation for the sintered glass beads assuming an exponential correlation for the frame bulk modulus variations. In (a) and (b), the correlation length is held fixed at $L = 1.6$ mm while the variance and the mean bulk modulus are increased. The variance is shown in the figures and the mean bulk modulus is $K_b = 1.009K_{b0}$ (long-dashed line), $K_b = 1.021K_{b0}$ (short-dashed line), and $K_b = 1.045K_{b0}$ (long-short dashed line). In (c) and (d), the variance and mean bulk modulus are held fixed at $\sigma_{bb}^2 = 0.14K_b^2$ and $K_b = 1.045K_{b0}$. The solid line in each figure is the prediction of Biot theory for the sintered glass beads with no variation in the bulk modulus and $K_{b0} = 4.23 \times 10^9$ Pa. In (a) and (c) the sound speed ratio is defined as the sound speed of the sediment normalized by the sound speed of the pore fluid.

Eq. (62) and any larger values of K_b and σ_{bb}^2 would only continue this trend.

For the sintered glass beads, however, significant changes to the sound speed and attenuation occur for relatively small changes in the variance as seen in Figures 4(a) and 4(b). For these values, the relation in Eq. (62) is easily satisfied, and the second-order perturbation theory is adequate to describe the mean field. In this case, since the unperturbed frame modulus is so much larger than for the SAX99 sediment, the fast and slow compressional wavenumbers are comparable in magnitude and the scattering from fast compressional waves into fast compressional waves occurs at only slightly higher frequencies than the fast wave to slow wave mode conversion. While the slow wave scattering contribution to the scattering levels out at $k_2 L \approx 10$, the fast wave scattering attenuation contribution causes the attenuation to continue increasing at a rate proportional to ω^2. In the region where the attenuation contributions from the two scattering mechanisms are comparable, the attenuation increases at a rate roughly proportional to ω. This is emphasized in Fig. 4(c) and 4(d) where the variance is held fixed and the correlation length is varied from $L = 0.8$ mm to $L = 16.6$ mm. Note that due to causality, this change in attenuation is also accompanied by a change in sound speed. As the slow wave scattering contribution levels out, so, too, does the sound speed. As the contribution to attenuation due to the scattering of fast waves increases, the sound speed begins to diverge as can be seen in the long-short dashed in Fig. 4(c) for $L = 16.6$ mm.

The second correlation function to examine is the von Kármán function,

$$C_{bb}(R) = s^{1-\nu}\Gamma^{-1}(\nu)(R/L)^{\nu}\,\mathrm{K}_{\nu}(R/L), \tag{65}$$

where K_ν is the modified Bessel function of the third kind, Γ denotes the gamma function, and ν is the Hurst coefficient which is assumed to be $0 < \nu \leq 1$. The three-dimensional Fourier transform of this correlation function yields the power spectrum,

$$W_{bb}(k) = \frac{\sigma_{bb}^2 L^3 \Gamma\left(\nu + \frac{3}{2}\right)}{\pi^{\frac{3}{2}}\Gamma(\nu)\left(1 + k^2 L^2\right)^{\nu+\frac{3}{2}}}. \tag{66}$$

When $\nu = 1/2$, the von Kármán function reduces to the exponential correlation function discussed above.

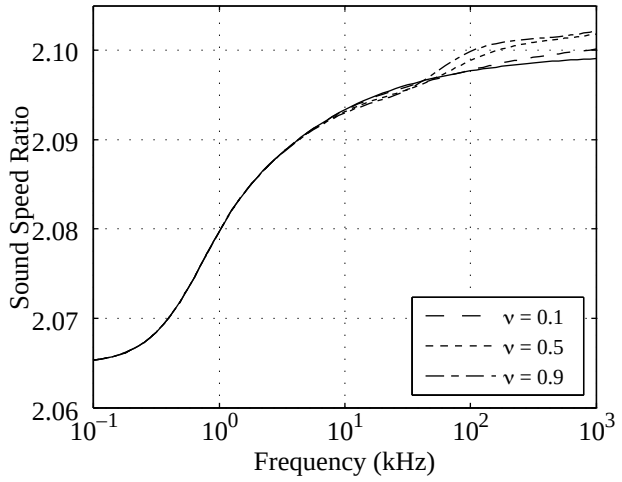

(a)

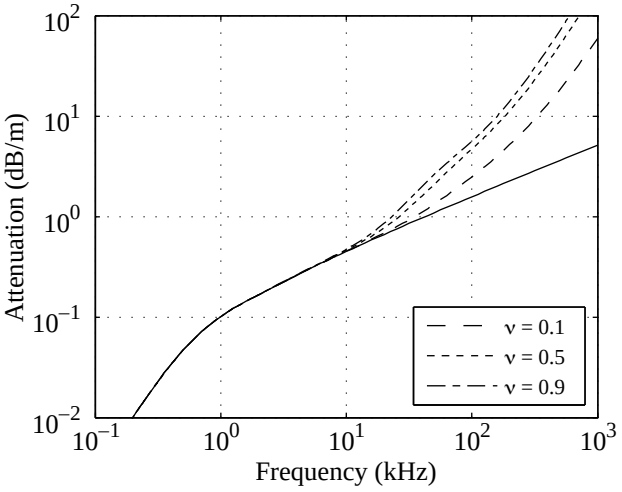

(b)

FIG. 5. Examples of (a) sound speed ratio and (b) attenuation for the sintered glass bead pack assuming a von Kármán function for the frame bulk modulus variations. The correlation length for each curve is held fixed at $L = 4.1$ mm, the variance is $\sigma_{bb}^2 = 0.14K_b^2$, and the mean bulk modulus is $K_b = 1.045K_{b0}$. The Hurst coefficient, ν, is $\nu = 0.1$ (long-dashed line), $\nu = 0.5$ (short-dashed line), and $\nu = 0.9$ (long-short dashed line). In (a) the sound speed ratio is defined as the sound speed of the sediment normalized by the sound speed of the pore fluid.

Unlike the exponential function, the von Kármán function does not allow for an analytical solution to the integral in Eq. (44). As a consequence, we will evaluate the integral numerically in the subsequent examples. Again, for the SAX99 sediment, the sound speed and attenuation are only weakly affected for values of K_b and σ_{bb}^2 for which the second-order perturbation theory applies. The variations in the sound speed and attenuation are on the same order as those observed in Fig. 3 for any value of ν. Therefore, we will focus on the sintered glass bead pack to examine how varying ν affects the propagating wave. Fig. 5 shows how the sound speed and attenuation are affected as ν is varied from 0.1 to 0.9. The curve for $\nu = 0.5$, the exponential function, is also plotted for comparison with the previous examples. Increasing ν above 0.5 has a minor effect on the attenuation, increasing the scattering contribution only slightly, while causing the associated dispersion to occur over a narrower band of frequencies. The opposite occurs as ν is decreased below 0.5. In this case, the scattering contribution to the attenuation decreases significantly as does the slope of the attenuation. The dispersion is also less pronounced as the sound speed changes over a much wider frequency band.

VI. DISCUSSION

In the introduction, we noted that for random packings of granular materials, such as sand grains, many simulations and experiments have observed the formation of force chains in the material. Along these force chains, a subset of the grains in the material carry a majority of the overburden pressure in the material. The close relationship between the contact forces between the grains and the frame moduli suggested that the frame moduli should also exhibit a random structure which could lead to scattering losses for waves propagating through the material.

However, for the Biot parameters measured for the SAX99 sediment, the effective frame modulus is very weak which is typical of sand sediments. In fact, a good approximation to the sound speed and attenuation (neglecting the anomalous high frequency behavior of the

attenuation) can be found if the frame moduli are set to zero as in the Effective Fluid Density Model (EDFM)[28]. It is not surprising, therefore, that assuming a heterogenous frame modulus for this sediment should not produce significant contributions to the dispersion or the attenuation due to mode conversion between the fast and slow compressional waves. For both the SAX99 and SAX04 measurements, as well as the laboratory measurements, the attenuation followed a linear frequency dependence and was larger at high frequencies than predicted by Biot theory. The additional attenuation due to the heterogenous frame modulus is therefore insufficient to account for this measured increase in attenuation.

These scattering contributions do, however, become significant for consolidated media, such as the sintered glass bead example, where the frame modulus is much larger. For the sintered glass beads, the frame modulus determined from experiments was found to be only an order of magnitude smaller than modulus of grains. For the SAX99 sediment, the frame bulk modulus was assumed to be at least three orders of magnitude smaller. For a poroelastic medium such as the glass beads, where the contacts have been fused together to form a fully consolidated structure, the force chains found in unconsolidated media are likely not present since the forces at the grain contacts have been allowed to relax during the melting process. The only source of heterogeneity in the frame modulus would have to be the structure of the porous frame itself and the local strength of this kind of porous frame is currently not well understood.

An intermediate case between these two extremes, where both force chains and a strong frame modulus may be present, could occur for a sediment under pressure. This could be the case for sand sediments tens of meters below the sediment/water interface. The overburden could produce significant contact forces between the grains leading to a large mean bulk modulus while the random packing of the grains would lead to heterogeneities in the frame modulus.

To determine if scattering from heterogeneities in the sediment might lead to the high frequency attenuation observed in the SAX99 and in the laboratory, it remains to apply the perturbed wave equation given in Eq. (28) to other heterogeneities in the Biot parameters

listed in Table I. Of particular interest should be those parameters for which the predictions of Biot theory are more sensitive and for which significant heterogeneities may be expected to occur. It is unlikely that the fluid parameters should vary significantly and, while the grains may exhibit some variation in their modulus and density, sorting due to wave action may lead to a suppression in the variation between the grains themselves. This suggests that those parameters which relate directly to the pore structure itself, specifically the permeability, tortuosity, and the porosity, may exhibit spatial variations which could lead to significant scattering. Work is currently underway to examine the predictions of the general perturbation theory given in Eq. (28) when the porosity of the sediment is heterogenous[32].

VII. CONCLUSIONS

In an effort to understand the role of heterogeneities in the propagation of high-frequency sound through an ocean sediment, we have applied perturbation theory to Biot's poroelastic equations. The resulting wave equation, while capable of modeling heterogeneities in any of the Biot parameters, was applied to the case of a randomly varying frame bulk modulus. The presence of the heterogeneities in the bulk modulus affects both fast and slow compressional wave propagation, but does not affect the propagation of shear waves. At low frequencies, the resulting mean wavenumber for the fast compressional wave reduces to the result presented previously by Müller and Gurevich for seismic propagation[16].

The effects of the frame modulus heterogeneities can be incorporated into a set of effective Biot coefficients each of which consists of the mean coefficient, a frequency-independent term that is a function of the frame modulus variance, and a frequency-dependent term that is a function of the frame modulus covariance within the medium. The frequency-independent term accounts for the softening of the medium due to the variations in the frame modulus, while the frequency-dependent accounts for scattering from the heterogeneities. For a propagating fast wave, when $k_2 L \approx 1$, mode conversion between the fast and slow waves scatters energy from the mean field increasing the attenuation of the mean

field. At higher frequencies, energy is also lost due to scattering from the coherent fast wave into incoherent fast waves. While the attenuation due to mode conversion levels off near $k_2 L \approx 10$, the attenuation due to fast wave scattering goes as ω^2.

The perturbation theory accounts for scattering up to second order in the modulus variations and was shown to be applicable to small variations in the bulk modulus. For weakly consolidated granular media, such as sand sediments, the mean frame modulus is typically much smaller than the grain or fluid modulus and the role of the variations in the frame modulus were shown to only weakly affect the sound propagation. For consolidated media, such as the sintered glass bead pack discussed here, weak variations in the frame modulus were shown to have a significant effect on sound propagation. Future work will explore the role of heterogeneities in parameters such as the porosity, which may have a more significant affect on propagation through weakly consolidated poroelastic media.

APPENDIX A: BIOT GREEN'S TENSOR

In order to apply perturbation theory to solve (16) with varying frame bulk and shear moduli, we need to know the Green's function which can be used to solve the inhomogenous poroelastic equation,

$$[\mathsf{K}_0]\,\nabla\left(\nabla\cdot\mathbf{U}\right)-[\tilde{\mu}_0]\,\nabla\times\left(\nabla\times\mathbf{U}\right)+ [\rho_0]\,\omega^2\mathbf{U}=-\mathbf{S}\left(\mathbf{r}\right). \tag{A1}$$

The inhomogenous equation with a point source,

$$[\mathsf{K}_0]\,\nabla\left(\nabla\cdot\mathfrak{G}\left(R\right)\right)-[\tilde{\mu}_0]\,\nabla\times\left(\nabla\times\mathfrak{G}\left(R\right)\right)+ [\rho_0]\,\omega^2\mathfrak{G}\left(R\right)=-\delta\left(\mathbf{R}\right)[\mathsf{I}]\;\mathfrak{I}, \tag{A2}$$

where $[\mathsf{I}]$ is the 2×2 identity matrix, $\mathfrak{I}$ is the identity tensor, and $R=|\mathbf{r}-\mathbf{r}'|$, has the

Green's tensor solution

$$\begin{aligned}\mathfrak{G}(R) = &\sum_{n=1}^{2} [\mathsf{G}_n] \nabla\nabla' g_n(R) \\ &- [\mathsf{G}_s] \nabla \times \nabla' \times (g_s(R)\mathfrak{I}) \\ &- [\rho_0]^{-1} \omega^{-2} \delta(R)\mathfrak{I},\end{aligned} \tag{A3}$$

where $n = 1$ and 2 is associated with the fast and slow wave, respectively, s is associated with the shear wave,

$$[\mathsf{G}_1] = \frac{[\mathsf{K}_0]^{-1} - [\rho_0]^{-1}\omega^{-2}k_2^2}{k_1^2 - k_2^2}, \tag{A4}$$

$$[\mathsf{G}_2] = \frac{[\mathsf{K}_0]^{-1} - [\rho_0]^{-1}\omega^{-2}k_1^2}{k_2^2 - k_1^2}, \tag{A5}$$

$$[\mathsf{G}_s] = \frac{[\hat{\mu}]}{\mu\rho^*\omega^2} + [\rho_0]^{-1}\omega^{-2}, \tag{A6}$$

$$g_m(R) = \frac{e^{ik_m R}}{4\pi R} \quad \text{where} \quad m = 1, 2, \text{or } s, \tag{A7}$$

$$[\mathsf{K}_0]^{-1} = \frac{\begin{bmatrix} -M & C \\ -C & H \end{bmatrix}}{(C^2 - HM)}, \tag{A8}$$

$$[\rho_0]^{-1} = \frac{\begin{bmatrix} -\rho^* & \rho_f \\ -\rho_f & \rho \end{bmatrix}}{\left(\rho_f^2 - \rho\rho^*\right)}, \tag{A9}$$

and

$$[\hat{\mu}] = \begin{bmatrix} 0 & 0 \\ 0 & \mu \end{bmatrix}. \tag{A10}$$

Note that the notation for the operators in (A3) differs from the notation of Morse and Feshbach who write them as $\nabla g_n(R)\nabla'$ and $\nabla \times g_n(R) \times \nabla'$. Morse and Feshbach illustrate the meaning of $\nabla\nabla' g_n(R)$ by operating with $\nabla\nabla' g_n(R)$ on some vector $\mathbf{f}(\mathbf{r}')$ which yields,

$$\begin{aligned}&f_x(\mathbf{r}')\nabla(\partial g/\partial x') + f_y(\mathbf{r}')\nabla(\partial g/\partial y') \\ &\qquad + f_z(\mathbf{r}')\nabla(\partial g/\partial z').\end{aligned} \tag{A11}$$

The other operator can be understood by writing it as

$$\nabla \times \nabla' \times \left(g_s\left(R\right)\mathfrak{I}\right) = \nabla\nabla' g_s\left(R\right) + \mathfrak{I}\nabla^2 g_s\left(R\right). \tag{A12}$$

Also note that

$$\nabla\nabla' g_n\left(R\right) = \left(\frac{1}{R}\frac{\partial g_n}{\partial R} - \frac{\partial^2 g_n}{\partial R^2}\right)\hat{\mathbf{R}}\hat{\mathbf{R}} - \frac{1}{R}\frac{\partial g_n}{\partial R}\mathfrak{I}, \tag{A13}$$

where $\hat{\mathbf{R}}$ is the unit vector in the direction of R.

If the source term in (A1) can be separated into longitudinal and tangential components,

$$\mathbf{S}\left(\mathbf{r}\right) = \nabla\Phi_S + \nabla \times \mathbf{\Psi}_S, \tag{A14}$$

the resulting field can be determined using the Green's tensor as

$$\begin{aligned}\mathbf{U}\left(\mathbf{r}\right) = &\sum_{n=1}^{2} k_n^2\left[\mathbf{G}_n\right]\nabla\int g_n\left(R\right)\Phi_s\left(\mathbf{r}'\right)d^3\mathbf{r}' + \\ &k_s^2\left[\mathbf{G}_s\right]\nabla\times\int g_s\left(R\right)\mathbf{\Psi}_S\left(\mathbf{r}'\right)d^3\mathbf{r}' + \\ &\frac{\left[\hat{\boldsymbol{\mu}}\right]}{\mu\rho^*\omega^2}\nabla\times\int\delta\left(R\right)\mathbf{\Psi}_S\left(\mathbf{r}'\right)d^3\mathbf{r}'.\end{aligned} \tag{A15}$$

Two relations that are used to simplify the perturbation solution are

$$\sum_{n=1}^{2}\left[\mathsf{G}_n\right]k_n^2 = \left[\mathsf{K}_0\right]^{-1} \tag{A16}$$

and

$$\sum_{n=1}^{2}\left[\mathsf{G}_n\right] = \left[\mathsf{\rho}_0\right]^{-1}\omega^{-2}. \tag{A17}$$

APPENDIX B: MEDIUM SOFTENING DUE TO MODULUS VARIATIONS

To understand the origins of the frequency independent term in the effective Biot coefficient matrix, Eq. (38), we consider the mean response of a poroelastic medium under static compression. For the heterogenous poroelastic medium we are considering, we will take the harmonic mean of the Biot coefficient matrix to determine the effective response of the medium,

$$\left[\mathsf{K}_{\mathsf{eff}}\right]^{-1} = \left\langle\left[\mathsf{K}\left(\mathbf{r}\right)\right]^{-1}\right\rangle. \tag{B1}$$

To see that this is equivalent to the self-consistent method for estimating the elastic constants in inhomogenous material discussed by Berryman[33], consider what happens if we replace the fluid in the poroelastic medium with a vacuum. In this case, the Biot coefficients reduce to $C = M = 0$ and $H(\mathbf{r}) = K_b(\mathbf{r}) + 4\mu_b/3$, $\rho_f = 0$, and the Biot equations reduce to the equations for an elastic medium. The harmonic mean of $H(\mathbf{r})$ becomes

$$\begin{aligned}\frac{1}{H_{eff}} &= \left\langle \frac{1}{H(\mathbf{r})} \right\rangle \\ &= \left\langle \frac{1}{K_b(\mathbf{r}) + \frac{4\mu_b}{3}} \right\rangle,\end{aligned} \tag{B2}$$

which is equivalent to Eq. (45) in reference [33].

With variations in the frame bulk modulus in the form of $K_b(\mathbf{r}) = K_{b0} + \delta K_b(\mathbf{r})$, we can approximate $[\mathsf{K}_{\mathsf{eff}}]$ by expanding $[\mathsf{K}(\mathbf{r})]^{-1}$ in a power series about K_{b0},

$$\begin{aligned}[\mathsf{K}(\mathbf{r})]^{-1} &= [\mathsf{K}_0]^{-1} + \frac{\partial [\mathsf{K}_0]^{-1}}{\partial K_b}\delta K_b(\mathbf{r}) \\ &\quad + \frac{1}{2}\frac{\partial^2 [\mathsf{K}_0]^{-1}}{\partial K_b^2}\delta K_b(\mathbf{r})^2,\end{aligned} \tag{B3}$$

where we have retained only those terms up to second order in δK_b.

The partial derivatives of the inverse Biot coefficient matrix in Eq. (B3) can be related to the partial derivatives of the Biot Coefficient matrix by

$$\frac{\partial [\mathsf{K}_0]^{-1}}{\partial K_b} = -[\mathsf{K}_0]^{-1}\frac{\partial [\mathsf{K}_0]}{\partial K_b}[\mathsf{K}_0]^{-1} \tag{B4}$$

$$\begin{aligned}\frac{\partial^2 [\mathsf{K}_0]^{-1}}{\partial K_b^2} &= -[\mathsf{K}_0]^{-1}\frac{\partial^2 [\mathsf{K}_0]^2}{\partial K_b}[\mathsf{K}_0]^{-1} \\ &\quad + 2[\mathsf{K}_0]^{-1}\frac{\partial [\mathsf{K}_0]}{\partial K_b}[\mathsf{K}_0]^{-1}\frac{\partial [\mathsf{K}_0]}{\partial K_b}[\mathsf{K}_0]^{-1}.\end{aligned} \tag{B5}$$

Substituting Eq. (B4) and (B5) into Eq. (B3) and taking the mean of the expansion gives

$$\begin{aligned}[\mathsf{K}_{\mathsf{eff}}]^{-1} &= [\mathsf{K}_0]^{-1} - \frac{1}{2}[\mathsf{K}_0]^{-1}\frac{\partial^2 [\mathsf{K}_0]}{\partial K_b^2}[\mathsf{K}_0]^{-1}\sigma_{bb}^2 \\ &\quad + [\mathsf{K}_0]^{-1}\frac{\partial [\mathsf{K}_0]}{\partial K_b}[\mathsf{K}_0]^{-1}\frac{\partial [\mathsf{K}_0]}{\partial K_b}[\mathsf{K}_0]^{-1}\sigma_{bb}^2.\end{aligned} \tag{B6}$$

To finally arrive at an expression for $[\mathsf{K}_{\mathsf{eff}}]$, we need to determine the inverse of Eq. (B6). To do this we will expand the inverse of the right side of Eq. (B6) as a function of the

variance about $\sigma_{bb}^2 = 0$. Upon doing this and using the relationship between the derivative of a matrix and the derivative of its inverse illustrated in Eq. (B4), we arrive at the final approximation for the effective Biot coefficients,

$$\begin{aligned}[\mathsf{K_{eff}}] &= [\mathsf{K}_0] - \frac{\partial [\mathsf{K}_0]}{\partial K_b} [\mathsf{K}_0]^{-1} \frac{\partial [\mathsf{K}_0]}{\partial K_b} \sigma_{bb}^2 \\ &\quad + \frac{1}{2} \frac{\partial^2 [\mathsf{K}_0]}{\partial K_b^2} \sigma_{bb}^2 \\ &= [\mathsf{K}_0] - \left([\mathsf{F_{b1}}] [\mathsf{K}_0]^{-1} [\mathsf{F_{b1}}] - \frac{1}{2} [\mathsf{F_{b2}}] \right) \sigma_{bb}^2. \end{aligned} \tag{B7}$$

This expression is identical to the frequency independent term in Eq. (38) determined from perturbation theory.

ACKNOWLEDGMENTS

This research was supported by the Office of Naval Research.

REFERENCES

[1] R. D. Stoll, "Marine sediment acoustics", J. Acoust. Soc. Am. **77**, 1789–1799 (1985).

[2] M. A. Biot, "Generalized theory of acoustic propagation in porous dissipative media", J. Acoust. Soc. Am. **34**, 1254–1264 (1962).

[3] M. A. Biot, "Mechanics of deformation and acoustic propagation in porous media", J. Appl. Phys. **33**, 1482–1498 (1962).

[4] E. L. Hamilton, "Geoacoustic modeling of the sea floor", J. Acoust. Soc. Am. **68**, 1313–1340 (1980).

[5] M. J. Buckingham, "Wave propagation, stress relaxation, and grain-to-grain shearing in saturated, unconsolidated marine sediments", J. Acoust. Soc. Am. **108**, 2796–2815 (2000).

[6] K. L. Williams, D. R. Jackson, E. I. Thorsos, D. Tang, and S. G. Schock, "Comparison of sound speed and attenuation measured in a sandy sediment to predictions based on the Biot theory of porous media", IEEE J. Ocean. Eng. **27**, 413–428 (2002).

[7] B. T. Hefner and K. L. Williams, "Sound speed and attenuation measurements in unconsolidated glass-bead sediments saturated with viscous pore fluids", J. Acoust. Soc. Am. **120**, 2538–2549 (2006).

[8] J.-X. Zhou, X.-Z. Zhang, and D. P. Knobles, "Low-frequency geoacoustic model for the effective properties of sandy seabottoms", J. Acoust. Soc. Am. **125**, 2847–2866 (2009).

[9] M. J. Buckingham, "On pore-fluid viscosity and the wave properties of saturated granular materials including marine sediments", J. Acoust. Soc. Am. **122**, 1486–1501 (2007).

[10] N. P. Chotiros and M. J. Isakson, "A broadband model of sandy ocean sediments: Biot–Stoll with contact squirt flow and shear drag", J. Acoust. Soc. Am. **116**, 2011–2022 (2004).

[11] S. R. Pride and J. G. Berryman, "Linear dynamics of double-porosity dual-permeability materials. I. Governing equations and acoustic attenuation", Phys. Rev. E **68**, 36603 (2003).

[12] S. R. Pride and J. G. Berryman, "Linear dynamics of double-porosity dual-permeability materials. II. Fluid transport equations", Phys. Rev. E **68**, 36604 (2003).

[13] Y. J. Masson and S. R. Pride, "Poroelastic finite difference modeling of seismic attenuation and dispersion due to mesoscopic-scale heterogeneity", J. Geophys. Res. **112**, B03204 (2007).

[14] S. R. Pride and Y. J. Masson, "Acoustic attenuation in self-affine porous structures", Phys. Rev. Lett. **97**, 184301 (2006).

[15] T. M. Müller and B. Gurevich, "A first-order statistical smoothing approximation for the coherent wave field in random porous media", J. Acoust. Soc. Am. **117**, 1796–1805 (2005).

[16] T. M. Müller and B. Gurevich, "Wave-induced fluid flow in random porous media: Attenuation and dispersion of elastic waves", J. Acoust. Soc. Am. **117**, 2732–2741 (2005).

[17] F. J. Karal and J. Keller, "Elastic, electromagnetic, and other waves in a random medium", J. Math. Phys. **5**, 537–547 (1964).

[18] C. Liu, S. Nagel, D. Schecter, and S. Coppersmith, "Force fluctuations in bead packs",

Science **269**, 513–515 (1995).

[19] H. A. Makse, G. Nicolas, D. L. Johnson, and L. Schwartz, "Granular packings: Nonlinear elasticity, sound propagation, and collective", Phys. Rev. E **70**, 061302 (2004).

[20] G. Mavko, T. Mukerji, and J. Dvorkin, *Rock Physics Handbook - Tools for Seismic Analysis in Porous Media* (Cambridge University Press, New York, NY) (2003).

[21] A. V. Anikeenko and N. N. Medvedev, "Structural and entropic insights into the nature of the random-close-packing limit", Phys. Rev. E **77**, 9 (2008).

[22] D. Tang, K. Briggs, K. Williams, D. Jackson, E. Thorsos, and D. Percival, "Fine-scale volume heterogeneity measurements in sand", IEEE J. Ocean. Eng. **27**, 546 (2002).

[23] N. P. Chotiros, "Biot model of sound propagation in water-saturated sand", J. Acoust. Soc. Am. **97**, 199–214 (1995).

[24] R. D. Stoll, "Comments on "Biot model of sound propagation in water-saturated sand" [J. Acoust. Soc. Am. **97**, 199–214 (1995)]", J. Acoust. Soc. Am. **103**, 2723–2725 (1998).

[25] N. P. Chotiros, "Response to: "Comments on 'Biot model of sound propagation in water-saturated sand' " [J. Acoust. Soc. Am. **103**, 2723–2725 (1998)]", J. Acoust. Soc. Am. **103**, 2726–2729 (1998).

[26] D. L. Johnson and T. J. Plona, "Acoustic slow waves and the consolidation transition", J. Acoust. Soc. Am. **72**, 556–565 (1982).

[27] D. R. Jackson and M. D. Richardson, *High-Frequency Seafloor Acoustics* (Springer, New York, NY) (2006).

[28] K. Williams, "An effective density fluid model for acoustic propagation in sediments derived from Biot theory", J. Acoust. Soc. Am **110**, 2276–2281 (2001).

[29] G. I. Block, "Coupled acoustic and electromagnetic disturbances in a granular material saturated by a fluid electrolyte", Ph.D. thesis, University of Illinois at Urbana-Champaign (2004).

[30] G. A. Gist, "Fluid effects on velocity and attenuation in sandstones", J. Acoust. Soc. Am. **96**, 1158–1173 (1994).

[31] S. M. Rytov, Y. A. Kravtsov, and V. I. Tatarskii, *Principles of Statistical Radiophysics*,

volume 4 (Springer, Berlin) (1989).

[32] B. T. Hefner, D. R. Jackson, and J. Calantoni, "The effects of scattering from heterogeneities in porosity during sound propagation through sand sediments.", J. Acoust. Soc. Am **125**, 2746–2746 (2009).

[33] J. G. Berryman, "Long-wavelength propagation in composite elastic media I. Spherical inclusions", J. Acoust. Soc. Am. **68**, 1809–1819 (1980).

TABLE I. Parameters used in calculating Biot results unless otherwise stated. The values in the column of parameters labeled "SAX99 Sand" correspond to the values in Table I of Ref. 6 for the best fit to the sound speed and attenuation measured during SAX99. Note that for the frame moduli, the imaginary parts have been removed and the moduli are assumed to be purely real. The values in the column of parameters labeled "Sintered Glass Beads" were determined from the parameters listed for the sintered glass bead sample B in Table III of Ref. 30.

Parameter	SAX99 Sand	Sintered Glass Beads
Porosity (β)	0.385	0.37
Mass density of sand grains (ρ_g)	2690 kg/m^3	2530 kg/m^3
Mass density of water (ρ_f)	1023 kg/m^3	1023 kg/m^3
Bulk modulus of sand grains (K_g)	3.2×10^{10} Pa	4.3×10^{10} Pa
Bulk modulus of frame (K_b)	4.36×10^{7} Pa	4.23×10^{9} Pa
Shear modulus of frame (μ_b)	2.92×10^{7} Pa	7.94×10^{9} Pa
Bulk modulus of water (K_f)	2.395×10^{9} Pa	2.395×10^{9} Pa
Viscosity (η)	0.00105 kg/m·s	0.00105 kg/m·s
Permeability (κ)	2.5×10^{-11} m^2	4.43×10^{-11} m^2
Tortuosity (α)	1.35	1.60

LIST OF FIGURES

FIG. 1 (a) Fast compressional sound speed and (b) attenuation determined from Eq. (41) with $[\mathsf{K}_{\mathsf{eff}}]$ given by Eq. (54) as a function of the variance, σ_{bb}^2, of the moduli variations normalized by K_{b0}^2. Both the sound speed and the attenuation have been normalized by their respective values when $\sigma_{bb} = 0$. These results were calculated for $f = 1$ kHz using the SAX99 sediment parameters in Table I while the value of the mean bulk modulus was increased from 4.36×10^7 Pa for the solid line, to 4.36×10^8 Pa for the short dashed line, and to 2.18×10^9 Pa for the long dashed line. 14

FIG. 2 Values of σ_{bb}^2/K_b^2 for which $[\mathsf{K}_{\mathsf{eff}}]$ remains equal to $[\mathsf{K}_0]$ for the SAX99 sediment parameters (solid line) and the sintered glass bead parameters (dash-dot line) as K_b is increased by three orders of magnitude. 16

FIG. 3 Examples of (a) sound speed ratio and (b) attenuation for the SAX99 sediment assuming an exponential correlation for the frame bulk modulus variations. The correlation length is held fixed at $L = 1$ mm while the variance and the mean bulk modulus are increased. The variance is shown in the figures and the mean bulk modulus is $K_b = 1.18K_{b0}$ (long-dashed line), $K_b = 1.41K_{b0}$ (short-dashed line), and $K_b = 2.04K_{b0}$ (long-short dashed line). In (a) the sound speed ratio is defined as the sound speed of the sediment normalized by the sound speed of the pore fluid. In (b) the lower set of curves is the contribution of the scattering from the fast compressional waves into the slow compressional waves to the attenuation of the mean fast compressional wave. The solid line in each figure is the prediction of Biot theory with no variation in the bulk modulus and $K_b = K_{b0}$. 21

FIG. 4 Examples of sound speed ratio and attenuation for the sintered glass beads assuming an exponential correlation for the frame bulk modulus variations. In (a) and (b), the correlation length is held fixed at $L = 1.6$ mm while the variance and the mean bulk modulus are increased. The variance is shown in the figures and the mean bulk modulus is $K_b = 1.009K_{b0}$ (long-dashed line), $K_b = 1.021K_{b0}$ (short-dashed line), and $K_b = 1.045K_{b0}$ (long-short dashed line). In (c) and (d), the variance and mean bulk modulus are held fixed at $\sigma^2_{bb} = 0.14K_b^2$ and $K_b = 1.045K_{b0}$. The solid line in each figure is the prediction of Biot theory for the sintered glass beads with no variation in the bulk modulus and $K_{b0} = 4.23 \times 10^9$ Pa. In (a) and (c) the sound speed ratio is defined as the sound speed of the sediment normalized by the sound speed of the pore fluid. 23

FIG. 5 Examples of (a) sound speed ratio and (b) attenuation for the sintered glass bead pack assuming a von Kármán function for the frame bulk modulus variations. The correlation length for each curve is held fixed at $L = 4.1$ mm, the variance is $\sigma^2_{bb} = 0.14K_b^2$, and the mean bulk modulus is $K_b = 1.045K_{b0}$. The Hurst coefficient, ν, is $\nu = 0.1$ (long-dashed line), $\nu = 0.5$ (short-dashed line), and $\nu = 0.9$ (long-short dashed line). In (a) the sound speed ratio is defined as the sound speed of the sediment normalized by the sound speed of the pore fluid. 25